Evaluation of The Antiproliferative Effect of Iso-Mukaadial Acetate on Breast and Ovarian Cancer Cells

Portia Raphela-Choma
University of Johannesburg
Mthokozisi Simelane
University of Johannesburg
Mpho Choene (mchoene@uj.ac.za)
University of Johannesburg

Research Article

Keywords: Breast cancer, Ovarian cancer, Anticancer, Apoptosis, Iso-mukaadial acetate

Posted Date: July 23rd, 2021

DOI: https://doi.org/10.21203/rs.3.rs-639116/v2

Version of Record: A version of this preprint was published at Advances in Traditional Medicine on February 5th, 2022. See the published version at https://doi.org/10.1007/s13596-022-00632-8.

Title: Evaluation of the antiproliferative effect of Iso-mukaadial acetate on breast and ovarian cancer cells

Portia P Raphela-Choma[1], Mthokozisi BC Simelane[2], and Mpho S Choene[1*]

Portia P Raphela-Choma: portiapheladi22@gmail.com

Mpho S Choene: mchoene@uj.ac.za, corresponding author*

Mthokozisi BC Simelane: msimelane@uj.ac.za

[1,1,2]Department of Biochemistry, University of Johannesburg (Auckland Park Campus), PO Box 524 Auckland Park 2006, South Africa.[1] portiapheladi22@gmail.com, [2] msimelane@uj.ac.za, [1*] mchoene@uj.ac.za

Abstract

Background: Natural compounds derived from various medicinal plants may activate several physiological pathways which can be valuable to diseases such as cancer. Isomukaadial acetate has previously been shown to possess antimalarial and anti-diabetic properties. The purpose of this study was to evaluate the antiproliferative effects of isomukaadial acetate on breast and ovarian cancer cell lines.

Method: Cell viability assays were conducted using AlamarBlue assay and xCELLigence system. Cell apoptosis and cell cycle arrest were determined and analyzed by flow cytometer. Effector caspase (3/7) activation was evaluated by caspase Glo®-3/7 reagent and gene expression was analyzed by Real-Time Polymerase Chain Reaction.

Results: The Alamar blue assay and xCELLigence showed that Iso-mukaadial acetate exhibited anti-proliferative effects on MDA-MB 231, RMG-1, and HEK 293 cell lines in a concentration-dependent manner. Iso-mukaadial acetate induced apoptosis in both cancer cell lines caused cell cycle arrest at the S phase (RMG-1) and early G2 phase (MDA-MB 231) and expressed caspase 3/7 activity in MDA-MB 231 and RMG-1 cells. BAX and p21 were upregulated in MDA-MB 231 and RMG-1 cells after treatment.

Conclusion: IMA significantly inhibited cancer growth and induced cell apoptosis with cell cycle modulation. IMA may be considered a promising candidate for the development of anticancer drugs either for its cytotoxic or cytostatic effect Furthermore, IMA requires to be further studied more to clearly understand its mechanism of action on cancer cells.

Keywords: Breast cancer; Ovarian cancer; Anticancer; Apoptosis; Iso-mukaadial acetate

Introduction

Breast cancer is one of the most occurring cancer in women around the world, with high occurrence rates in well-established countries. It is documented to be the second leading cause of death rate in women worldwide **(1)**. Breast cancer does not affect women only, but it can occur in men including transgender **(2)**. Ovarian cancer is a lethal disease that affects 1-2 % of females and about 20,000 new cases are identified yearly with 130,000 deaths globally. It is documented that the occurrence rate of ovarian cancer has increased

over time affecting most people in developed countries. Ovarian cancer is the 6th most occurring cancer affecting females all over the world and the 5th cause of death **(3)**. Apoptosis is a programmed cell death that is caused by the expression of explicit genes to remove damaged cells, for instance during cell development. Apoptosis is induced by DNA damage in precancerous lesions and other factors, which removes the harmful cells thereby blocking the development or growth of a tumour. Since cancer cells are reported to be resistant to apoptosis, better therapeutic approaches need to be implemented to reestablish cancer cell's sensitivity to apoptosis (**4**).

Medicinal plants have continued to be substantial hope for drug discovery and development in various diseases. Natural plants have been and still are explored as vital resources for cancer therapies including therapies for other diseases such as diabetes, malaria. Medicinal plants are used by approximately 70 % of the world as a source for potential drug agents (**5**) and about 70-95 % of people in the developing countries use traditional medicinal plants for health care services (**6**). Different cultures across the world have been acquiring knowledge, skills, and practice of using medicinal plants in diagnosis, prevention, and treatment of infections/diseases before the development of western medicine/pharmaceutical industries (**7**). Natural compounds derived from various medicinal plants may activate several physiological pathways which can be valuable to diseases such as cancer. Previous studies have reported that natural compounds have a positive impact on the health benefits of people by targeting specific genes or metabolic pathways. They can effectively reduce side effects such as nausea, fatigue, and anemia coming from chemotherapy or other cancer treatments and advance the existing and survival rates of patients (**8**) and have minimal toxicity (**9**).

Previous studies have shown that iso-mukaadial acetate, a drimane sesquiterpenoid possesses antimalarial and anti-diabetic properties (**10**)**,** (**11**), (**12**). This compound was isolated from a South African plant (*Warburgia salutaris*) that is extensively used for the treatment of bronchitis, ulcers, and oral thrush (**13**), (**14**). The plant is also recommended by traditional healers in treating and managing cancer (**15**)**,** (**14**). In this study, isomukaadial acetate (IMA) was evaluated for its antiproliferative activities on breast and ovarian cancer cell lines, which triggered cell apoptosis by the expression of cell apoptotic

genes and cell cycle arrest. Note, this is the first findings of the anti-proliferative effect of is-mukkadial acetate on cancer cell lines.

Materials and method

Reagents

Iso-mukaadial acetate was previously isolated from the University of KwaZulu Natal by Simelane and colleagues. Breast cancer (MDA-MB 231) cell lines and normal embryonic kidney (HEK293) cell lines were donated by Dr. Engelbrecht Z (University of Witwatersrand). The RMG-1 cell lines were donated by Prof Motadi LR (University of Johannesburg). Dulbecco's Modified Eagle's medium (DMEM) and trypsin were manufactured by LONZA (RSA). Dulbecco's phosphate-buffered saline (DPBS) was manufactured by HyClone, GE Healthcare. AlamarBlue cell viability reagent was manufactured by Invitrogen, Thermo Fischer Scientific. Trypan blue (0.4 %) was manufactured by LONZA (RSA). Staurosporine was obtained from Prof Motadi (University of Johannesburg) and etoposide from Sigma. Fetal bovine serum (FBS) was manufactured by HyClone, GE Healthcare. Caspase-Glo® 3/7 assay was manufactured by Promega (USA). Relia-Prep RNA cell miniprep kit was manufactured by Promega (USA). Propidium Iodide was manufactured by Sigma (USA) and Annexin V/FITC +PI was manufactured by R&D System (USA).

Preparation of the compound

The Iso-mukaadial acetate (IMA) was weighed separately and dissolved in DMSO to a stock concentration of 10 mM. The compound was stored at 4 °C until use.

Cell culture

The HEK 293, MDA-MB 321, and RMG-1 cell lines were maintained in 75 cm2 and 25 cm2 cell culture flasks under the following conditions:37 °C, 5 % CO2, and 95 % humidity atmosphere in an incubator. The human cell lines were grown until they reached a confluency of about 70 % to 80 % using DMEM supplemented with 10 % fetal bovine serum and 1 % penicillin-streptomycin. When the cancer cell lines reached 70-80 %

confluency, the cells were washed with 1X DPBS and exposed to 1X trypsin-EDTA for less than 1 minute (depend on the type of cell line). After incubation with trypsin, a 10 % FBS media was added into a flask to deactivate trypsin, then the mixture was transferred into a 50 ml falcon tube and centrifuged for 4 minutes at 2200 x g. The cell viability concentration was determined by using 0.4 % of trypan blue. From the 50 ml falcon tube containing cells with media, 20 µl of cells were mixed with 20 µl of 0.4 % of trypan blue. The mixture was aspirated gently, then 10 µl of the mixture was spread on the cell counter slide using a micropipette and the number of viable cells was counted using the TC20 Automated Cell Counter.

Cell proliferation assay using AlamarBlue

Firstly, the cell lines were grown in an incubator (with the same conditions mentioned in 2.3) until 80 % of cell confluence was reached. After the cell lines were sub-cultured and seeded in 96 well plates. Trypan blue was used to check the viability of the cells. The desired concentration of cells used was 5.0 x 104 for the HEK293 cell line, 1.0 x 104 for MDA-MB 321 and RMG-1, then a total of 100 µl of cells/ml was seeded on the 96 well plates for 24 hours. After 24 hours of incubation, the cell lines were treated with different concentrations of the compounds namely, 5 µM, 2.5 µM, 1.25 µM, and 0.65 µM for IMA for 24 hours. Positive control was etoposide at a concentration of 100 µM. Negative control was DMSO with cells (0.1%) cells with media only. After 24 hours, 10 µl of AlamarBlue was added to each well in the dark, then the plates were wrapped with aluminum foil as the dye is sensitive to light and incubated for 2 hours. After 2 hours of incubation, the plates were read by a fluorescence microplate reader (Synergy HT).

Real-time cell viability analysis using xCELLigence system

The xCELLigence RTCA was placed in 37 °C, 5 % CO2, and a 95 % humidified incubator and was calibrated before use. Different cell concentrations for MDA-MB 321, RMG-1 and HEK 293 cell lines (1 x 104 cell/ml, 5 x 104 cell/ml and 1.5 x 105 cell/ml) were seeded on the E16 well plates for 22 hours. The cell lines were left for 30 minutes to allow cell attachment before running the RTCA system. After 22 hours, the cell lines were treated with different compound concentrations: IMA (10, 5, 2.5, 1.3, 0.6 µM) for 3 days. A 0.1 %

was used as negative control and 100 µM etoposides were used as a positive control which was run in duplicates including the different compound concentrations. Etoposides, MA, and DMSO were dissolved in DMEM media before treating the cells. The RTCA was supervised every 15 minutes and the results were recorded by the RTCA software.

Apoptosis assay using Annexin V + FITC and PI

The cell lines were seeded into Petri dishes MDA-MB 231 (2 x 105) and RMG-1 (2 x 105) for 24 hours. The cell lines were then treated with the IC50 of iso-mukaadial acetate for 24 hours. Then the treated cells plus media were transferred into 2 ml Eppendorf tubes, washed with DPBS, and the remaining attached cells in the Petri dishes were trypsinized. The control cells were resuspended in fresh media after trypsinization to recover in an incubator. The trypsinized cells were transferred in the same Eppendorf tubes. The mixtures were micro-centrifuged at 500 x g for 2-5 minutes. Following the manufacturer's protocol, the supernatants were removed, and the pellets were washed twice with icecold DPBS at 500 x g for 2-5 minutes depending on the cell line. The binding buffer (1x) was prepared with autoclaved distilled water and 90 µl of it was added into different Eppendorf's containing the cell including 5 µl of Annexin V/FITC and 5 µl PI to make a final volume of 100 µl. The mixtures were vortexed and incubated in the dark on ice for 15 minutes. About 300 µl of the binding buffer was added into the flow tubes containing the cells and the dyes before reading the results. A flow cytometer (BD FACS AriaTm II) was then used to measure apoptosis.

Cell division cycle using Propidium Iodide

In this study, the cells were counted using a T20 cell counter of about 1x105 to 1x106 depending on the cell line. The cell lines were seeded in small Petri dishes respectively and incubated for 24 hours. The plated cells were treated with both compounds respectively using the IC50 obtained. The media was decanted into the Eppendorf tubes. Trypsin was added into the Petri dishes to detach the remaining cells and poured off into the same Eppendorf tubes. The mixture in the Eppendorf tubes was centrifuged at 300 x g for 3 minutes and decanted the supernatant. Cells were washed with ice-cold 1x DPBS (500 ul), before pouring off, they were centrifuged at 300 x g for 3 minutes and carefully

poured off the supernatant. The cells were fixed in cold 0.5 ml (500 ul) 70% absolute ethanol at 4 °C and incubated overnight or stored at -20 °C for several days until use. After incubation, the cell samples were centrifuged at 500 x g for 5 minutes, washed cells with cold 1X PBS twice, and centrifuged at 500 x g for 3 min. Cells have treated the cells with RNase A by adding 5 ul of 10mg/ml solution followed by 300 ul of PI (10 mg/ml) and incubated for 30 minutes on ice in the dark until read by flow cytometer (BD FACS AriaTm II).

Caspase-Glo® 3/7 activity

Following the manufacture's protocol from Promega, caspase-Glo® 3/7 assay was used to measure the activation of caspase 3/7 in MDA-MB 231 and RMG-1 cell lines after treatment with IC50 of iso-mukaadial acetate. MDA-MB 231 (2 x 105) and RMG-1 (2 x 105) cell lines were seeded in the 96 well microplates for 24 hours. The cell lines were treated with iso-mukaadial acetate IC50 values for 24 hours. The caspase-Glo® reagent was then added to the wells and incubated on the shaker for 30 minutes. The caspase activities were measured by a luminescence microplate reader (Synergy HT) and the results were represented as Relative Luminescence Units.

RNA extraction using Relia-Prep™ RNA-cell miniprep kit

Following manufacturers protocol from Promega, RNA was extracted from MDA-MB 231 and RMG-1 cell lines using Relia-Prep™ RNA-cell miniprep kit after treatment with IMA IC50. The three cell lines were harvested before cell lysis, then collected cells in an Eppendorf tube by microcentrifugation at 300 x g for 5 minutes. The cell pellets were washed with ice-cold 1X DPBS and microcentrifuge at 300 x g for 5 minutes. The supernatant was discarded. The BL-TG Buffer mixture was prepared and about 100 µl was added to the pellets respectively, then vortexed. About 35 µl of isopropanol was added to the mixture and vortexed for 5 seconds. Aseptically, the cell lysates were transferred into a Minicolumn in a collection tube and were microcentrifuge at 13,000 x g for 30 seconds. About 500 µl of RNA wash solution was added to the Minicolumn and microcentrifuge at 13,000 x g for 30 seconds. DNase I incubation mixture was prepared and 30 µl of the mixture was added into each Minicolumn tubes and incubated at room

temperature for 15 minutes. Column wash solution (200 µl) was added after the incubation period and microcentrifuge at 13,000 for 15 seconds. The RNA wash solution was added and microcentrifuge at a higher speed for 2 minutes. The Minicolumn was transferred into an elution tube and nuclease-free water was added, microcentrifuge at 13,000 x g for 1 minute. The extracted RNA was quantified by determining its purity using Nano-Drop and an A260/A280 ratio of 2.0 was considered as pure. Then the RNA was stored at -80 °C until further use.

Real-Time Polymerase Chain Reaction using SYBR Green

After mixing the following components (RNA template, primers, random primers), the mixture was incubated at 70 °C using a master-cycler gradient for 5 minutes. Then the mixture was chilled on ice immediately for 5 minutes, vortexed for 10 seconds, and chilled on the ice again until the reverse transcription mixture is added. The reverse transcription mixture was combined with the 5 µl of RNA and the primers. Then the cDNA synthesis conditions were applied, and the synthesized cDNA was stored at -80 °C until further use. The amplification of cDNA was done using GoTaq G2 Green master mix 2X. The cycle conditions were repeated 40 times and the samples were held at 4 °C for several hours before the amplicons were visualized on agarose gel electrophoresis. The iTaq™ Universal SYBR® Green Supermix, primers, and cDNA were used. The components above were mixed by vortexing for few seconds and stored on ice in the dark until further use. A CFX96-connect machine was used to run real-time PCR and the following thermal cycling was programmed.

Statistical analysis

Results were analyzed statistically by using Graph Pad Prism, ModFit LT and REST 2007 software. The data were expressed as mean ± Standard Deviation (*$P < 0.05$, **$P < 0.01$ ***$P < 0.001$). A p-value less than 0.05 ($p < 0.05$) was considered as significant.

Results

The results below represent the anti-proliferative effects of Iso-mukaadial acetate (IMA) at various concentrations on breast cancer, ovarian cancer, and embryonic kidney normal

cell lines. As shown in Figures 1,5 and 6, IMA exhibited anti-proliferative effects on MDAMB 231, RMG-1, and HEK 293 cell lines stained/treated with the AlamarBlue reagent (endpoint assay). Real-time cell analysis (xCELLigence) has also shown the inhibitory effects of IMA on the cells (figure 1, 5, 6). IMA induced apoptosis, cell cycle arrest (2 and 7), and the activation of caspase 3/7 (figure 3 and 8) was also observed. The expression of selected genes was determined as shown in Figures 4 and 9. IMA may be a promising anticancer agent in the future on cancer cell lines.

Anti-proliferative effect of IMA using Alamarblue and xCELLigence system on MDA-MB 231 cells

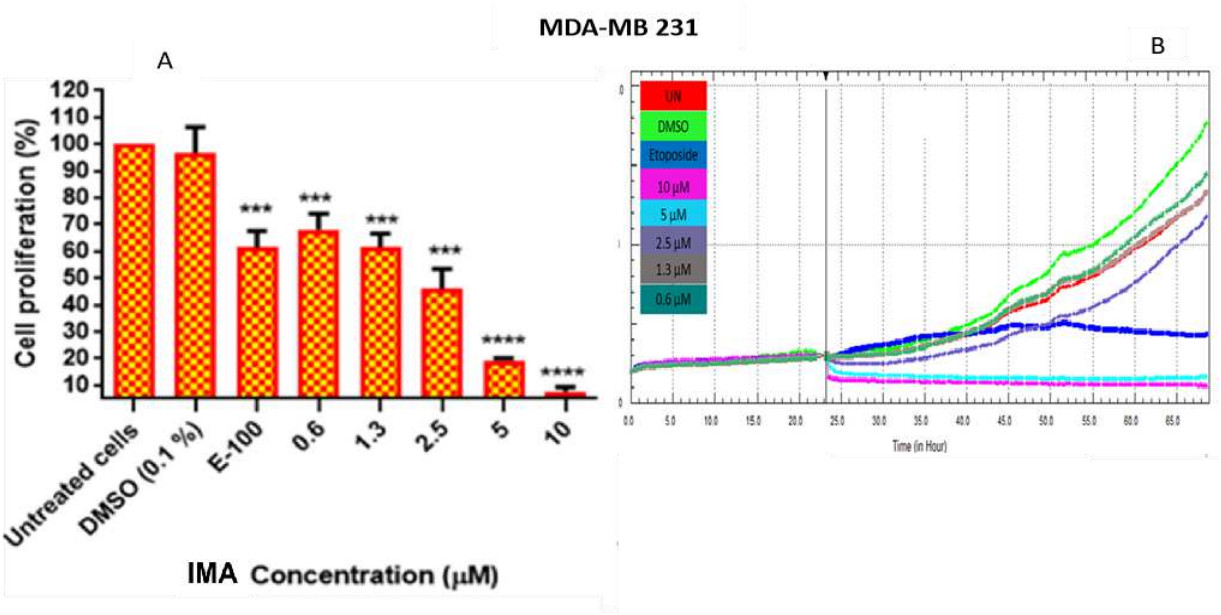

Figure 1A and B: The anti-proliferative effect of IMA on MDA-MB 231 cell line using (A) endpoint assay (24 hours) and (B) real-time cell analyzer (over 48 hours) to monitor the effectiveness of IMA. A decline in cell proliferation was observed in a concentrationdependent manner. At higher concentrations, IMA showed to be highly toxic in comparison with etoposide. Low concentrations showed that IMA was moderately cytotoxic within 24 hours of treatment (1B). DMSO (0.1 %) showed to promote cell proliferation in comparison to untreated control. The data were expressed as mean ± Standard Deviation (*P < 0.05, **P < 0.01 ***P < 0.001, ****P < 0.0001) from three biological repeats.

Apoptotic induction and cell cycle arrest using Flow cytometer on MDA-MB 231 cells

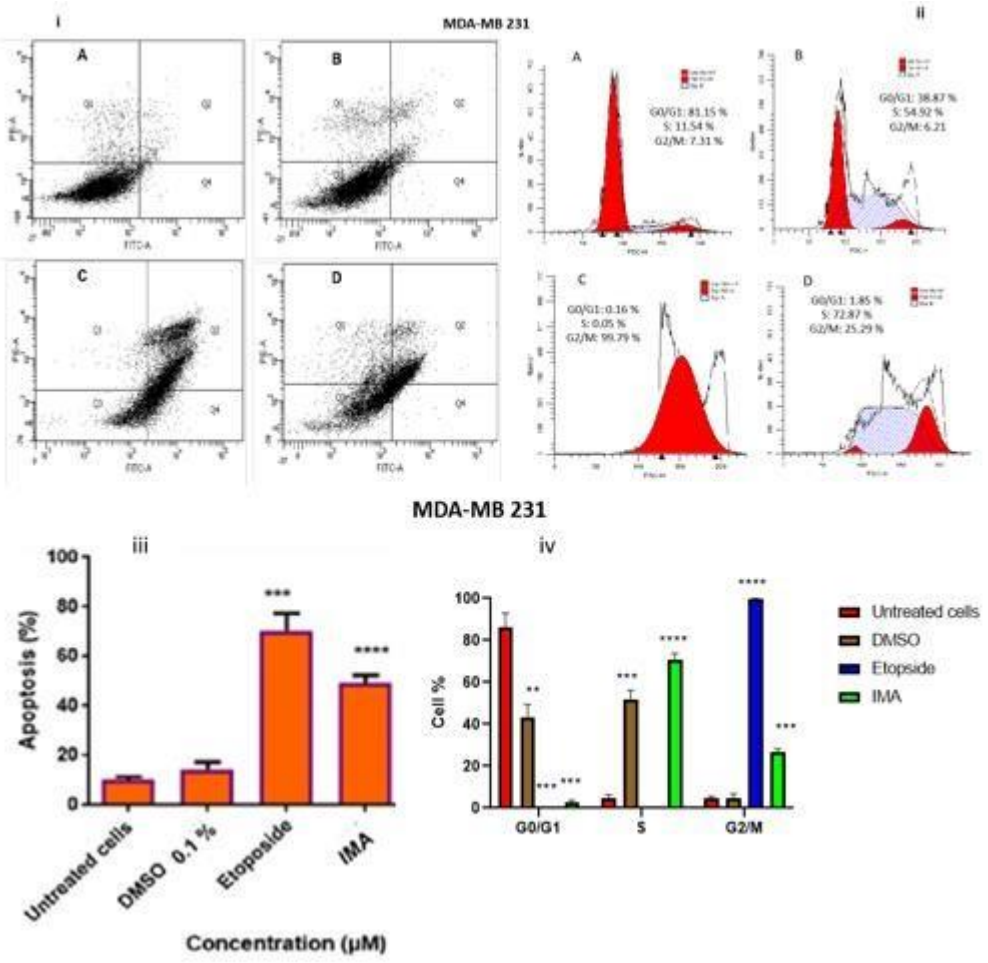

Figure 2: Cell apoptosis (i) and cell cycle arrest results (ii) were analyzed following the treatment with IMA including positive control etoposide on MDA-MB 231 cell lines after 24 hours. A (untreated cells), B (DMSO 0.1 %), C (Etoposide 100 µM), D (IMA 2.7 µM). the results obtained were read and analyzed by flow cytometer and ModFit LT 5.0 software. The overall percentages of cell apoptosis (iii) induced by IMA was low in comparison to etoposide. Cell cycle (iv) results exhibited that etoposide caused G2/M phase (99 %) arrest while IMA caused S phase (72 %) and early G2 phase (25 %) cell cycle arrest. The data were expressed as mean ± Standard Deviation (**P < 0.01 ***P < 0.001, ****P < 0.0001) from three biological repeats.

Activation of caspase 3/7 using caspase 3/7 Glo reagent on MDA-MB 231 cells

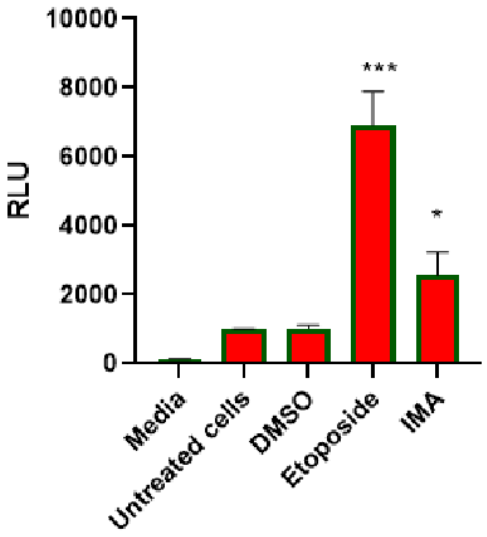

Figure 3: Caspase 3/7 activation modulated by the biological activity of IMA on the MDAMB 231 cell line. The cells were treated with IMA IC_{50} (2.7 µM) for 24 hours. Caspase 3/7 activity was analyzed by luminescence. Etoposide expressed a high level of caspase activity than IMA. These results correlate with figure 2 results. The data were expressed as mean ± Standard Deviation (*P < 0.05, ***P < 0.001) from three biological repeats.

Gene expression using real-time PCR

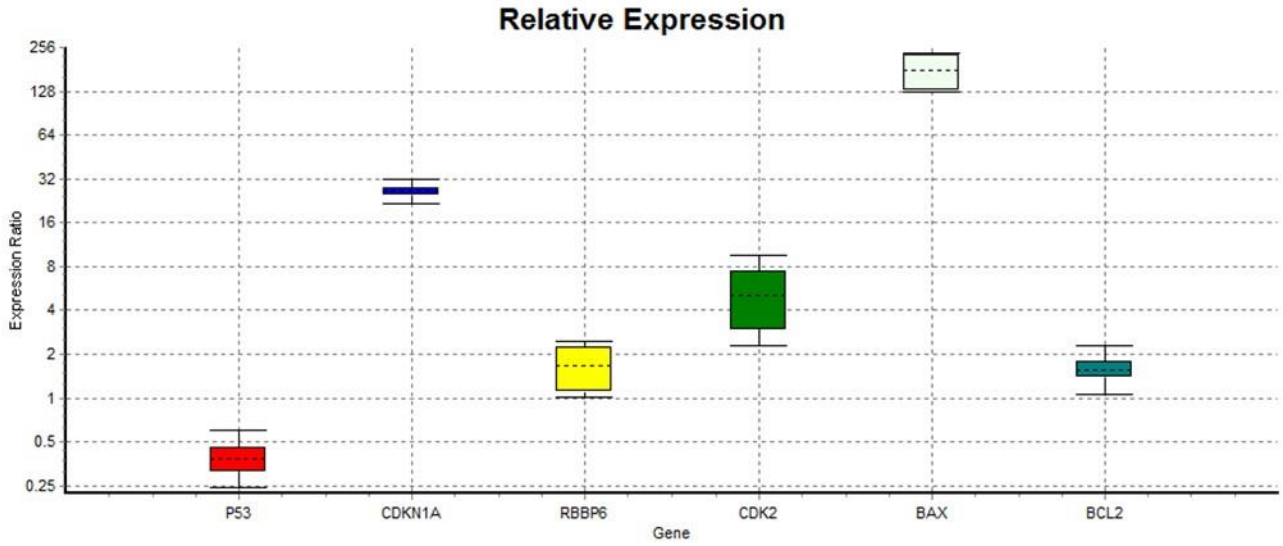

Figure 4: Real-time PCR results were analyzed using REST 2007 software. The following box plots represent MDA-MB 231 cell line gene expression after a 24-hour treatment with IMA. GAPDH was used as a reference gene. The data were expressed as mean ± Standard Deviation from two biological repeats.

Anti-proliferative effect of IMA using Alamarblue and xCELLigence system on HEK 293 cells

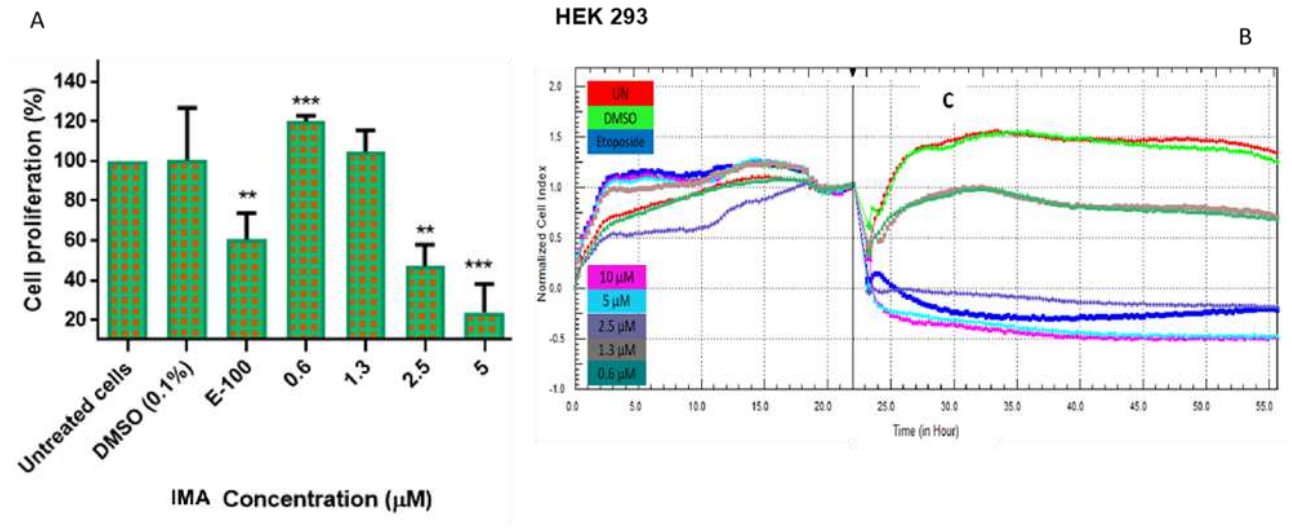

Figure 5: The cytotoxic effect of IMA on HEK 293 cell line using (A) endpoint assay (24 hours) and (B) real-time cell analyzer (over 48 hours) to monitor the activity of IMA on non-cancer cells. Higher concentrations of IMA were toxic to the HEK 293 cells in comparison to low concentrations. The cytotoxic effect of etoposide was also observed. DMSO did not have any effect on the HEK 293 cells in comparison to untreated cells and IMA response. The data were expressed as mean ± Standard Deviation (*P < 0.05, **P < 0.01 ***P < 0.001, ****P < 0.0001) from three biological repeats.

Anti-proliferative effect of IMA using Alamarblue and xCELLigence system on RMG-1 cells

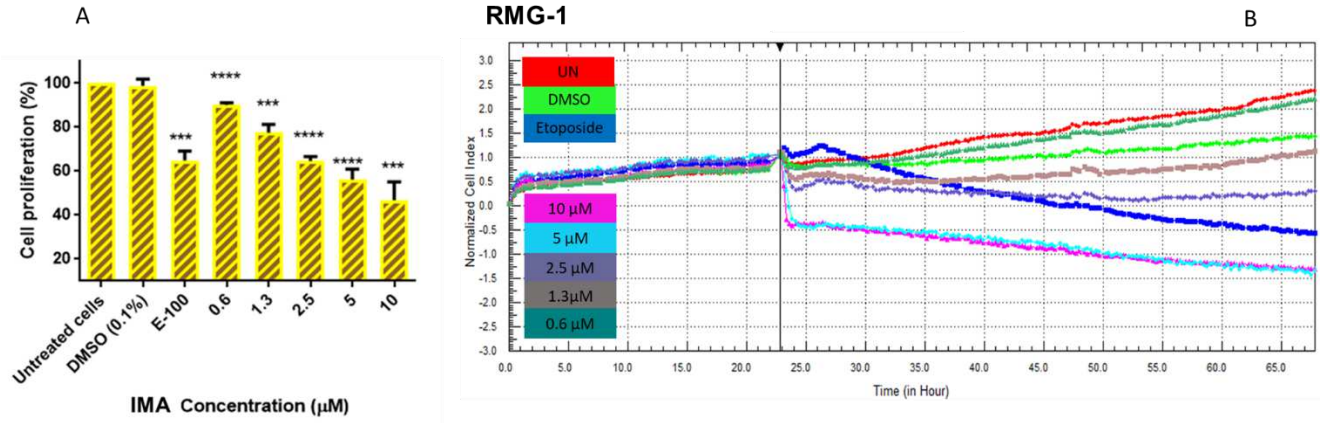

Figure 6: The cytotoxic effect of IMA on RMG-1 cell line using (A) endpoint assay (24 hours) and (B) real-time cell analyzer (over 48 hours) to monitor the activity of IMA. A decline in cell proliferation was observed in a concentration-dependent manner. At higher concentrations, IMA showed to be highly toxic in comparison with etoposide. Low concentrations showed that IMA was moderately cytotoxic within the few hours of treatment (6B). DMSO (0.1 %) showed to slow down cell proliferation in comparison to untreated control. The data were expressed as mean ± Standard Deviation (*P < 0.05, **P < 0.01 ***P < 0.001, ****P < 0.0001) from three biological repeats.

Apoptotic induction and cell cycle arrest using Flow cytometer on RMG-1 cells

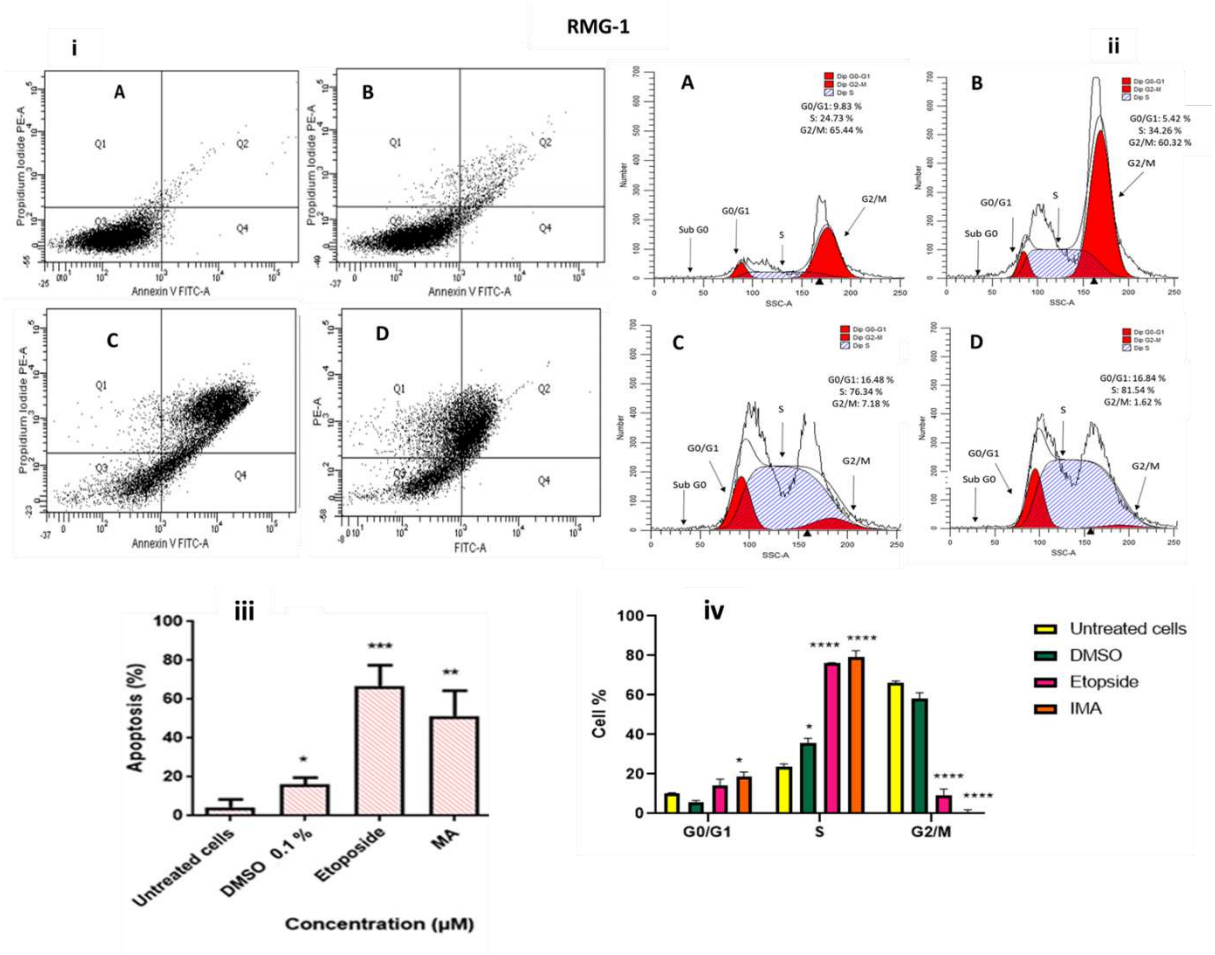

Figure 7: Cell apoptosis (i) and cell cycle arrest results (ii) were analyzed following the treatment with IMA including positive control etoposide on RMG-1 cell lines after 24 hours. A (untreated cells), B (DMSO 0.1 %), C (Etoposide 100 µM), D (IMA 2.3 µM). The results obtained were read and analyzed by flow cytometer and ModFit LT 5.0 software. The

overall percentages of cell apoptosis (iii) and cell cycle (iv) results. IMA and etoposide induced cell apoptosis. Etoposide caused S phase (76 %) arrest while IMA caused S phase (81 %) cell cycle arrest with a decrease in cell population in other phases. The data were expressed as mean ± Standard Deviation (*P < 0.05, **P < 0.01 ***P < 0.001) from three biological repeats.

Activation of caspase 3/7 using caspase 3/7 Glo reagent on RMG-1 cells

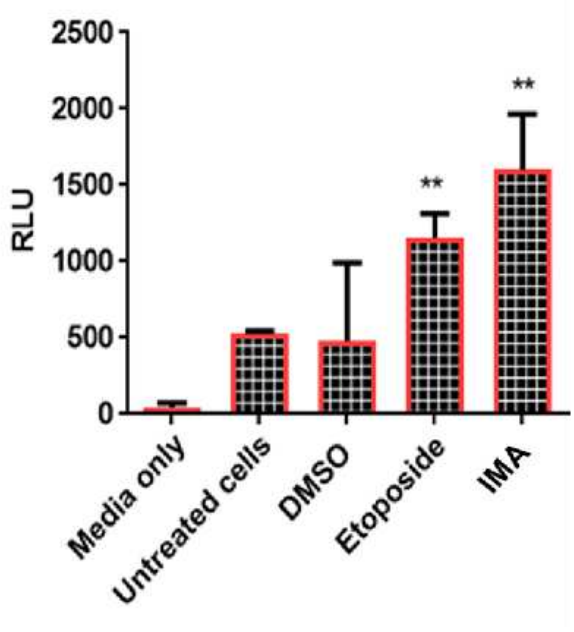

Figure 8: Caspase 3/7 activation modulated by the biological activity of IMA on the RMG1 cell line. The cells were treated with IMA IC_{50} for 24 hours. Caspase 3/7 activity was analyzed using luminescence. A high expression of caspase 3/7 was observed in comparison with etoposide and these results correlate with figure 7 results. The data was expressed as mean ± Standard Deviation (*P < 0.05, ***P < 0.001) from three biological repeats.

Gene expression using real-time PCR

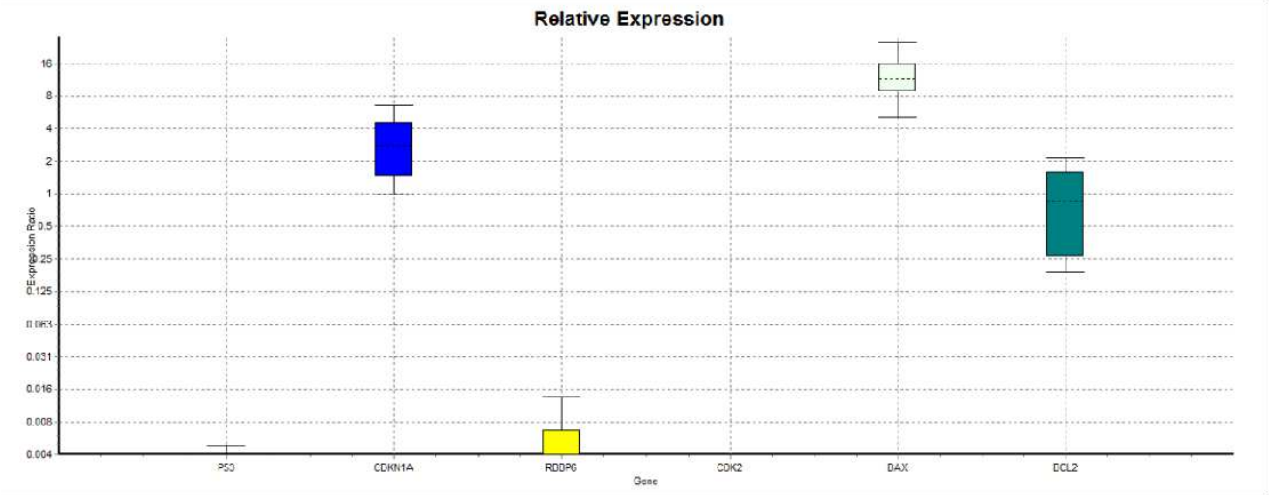

Figure 9: Real-time PCR results were analyzed using REST 2007 software. The following box plots represent RMG-1 cell line gene expression after a 24-hour treatment with IMA. GAPDH was used as a reference gene. The data were expressed as mean ± Standard Deviation from two biological repeats.

Discussion

Natural compounds derived from medicinal plants are promising to advance the development and treatment efficacy in human cancer cells (**16**). Researchers are moving towards natural compounds due to the gene mutations and cancer-causing properties of the synthesized compounds (**17**). The anti-proliferative effect of IMA was evaluated using Alamar-blue (endpoint assay) and xCELLigence system (real-time cell analyzer). We found that IMA significantly exhibited an anti-proliferative effect on MDA-MB 231 and RMG-1 cells in a concentration-dependent manner. The cytotoxic effect of IMA on cancer cell lines in comparison with non-cancer cells (HEK 293) exhibits that IMA is significantly selective based on the type of cell line. Etoposide (positive control) in both endpoint assay and real-time cell analysis exhibited a cytotoxic effect on the MDA-MB 231, RMG-1, and HEK 293 cells at higher concentrations (100 µM) and it was not selective on the cell lines in comparison to IMA.

The endpoint assay (Alamar-blue, figure 1A) showed the cytotoxic effect of IMA on the cancer cells in a concentration-dependent manner after 24 hours of treatment. In realtime cell viability analysis (figure 1B), IMA exhibited an inhibitory effect on the MDA-MB 231 cell lines over 48 hours of treatment. The real-time cell analyzer results, exhibit that MDA-MB 231 was resistant to treatment within the first 24 hours of treatment. This may be an interesting point because at 10 and 5 µM concentrations, the cells lost their viability, hence a decline in cell proliferation was observed. This exhibits the toxicity of IMA at higher concentrations with the possibility of apoptosis induction. At lower concentrations (2.5, 1.3, and 0.6 µM), figure 1B, showed that IMA may have slowed down/ inhibited cell proliferation and growth within the first few hours after treatment. This revealed that IMA may not be toxic at lower concentrations but suggesting that IMA may act as a cytostatic compound that inhibits cellular proliferation at low concentrations (**18**). Nonetheless, after the first 24 hours (after treatment), a rise in recovery and cell proliferation of MDA-MB 231 cells was observed. It may be that MDA-MB 231 formed a resistance mechanism towards the compound (**19**), after a certain period of exposure which is what cancer cells do to defend themselves. This result reveals the understanding and importance of shorter and longer drug agent exposure to cells. Even so, the activity of IMA based on the results

obtained is highly efficient as compared to the activity of etoposide. By analyzing the realtime cell proliferation results, IMA cytotoxic/cytostatic effect on MDA-MB 231 requires further evaluation to understand its effect on breast cancer cells.

Furthermore, the results in Figures 2i and iii, exhibited that IMA induced cell apoptosis on MDA-MB 231 cell lines at IC_{50} (2.7 µM). Etoposide showed a higher apoptotic rate than IMA as shown in figure 2i. This observation may correlate with results obtained in figure 1B. Again, the caspase 3/7 results attest to this as IMA expressed caspase 3/7 in low proportions as compared to etoposide. The upregulation of BAX exhibit that some percentages of cells were damaged beyond repair and were signaled to undergo apoptosis (see figure 4) hence figure 2i and iii were observed. It was documented that the p53-independent pathways result in apoptotic response using other alternative death pathways, upregulating BAX and p21 expressions (**20**). In a previous study, the p53independent apoptotic pathway was also observed in MCF-7 and T47D cell lines as the p53 response was found to be the same after treatment (**21**).

Using flow cytometric analysis of propidium iodide stain (figure 2 ii and iv), IMA was assessed its effect on cell cycle progression on MDA-MB 231 cells. Cell cycle arrest is the response to DNA damage or cellular stress. After 24 hours treatment, the number of cells in the GO/G1 phase was very low and a significant increase in the number of cells in the S phase was observed, with reductions of cell population in the G2/M phase. The cell cycle results indicated that IMA encouraged cell cycle arrest in the S-phase and early G2 phases. The arrest in the S phase may relate to the induction of p21 expression observed in figure 4. This observation suggested that IMA may have prevented the DNA replication process and arrested cells in the S phase. Nonetheless, low expression of CDK2 was observed and this may have slightly delayed the S phase to G2 phase progression (**22**) as about 25 % of G2/M phase cell populations were observed. IMA may possess the ability to cause cell cycle arrest by inhibiting DNA synthesis and cause DNA damage leading to G2 arrest (**23**).

IMA reduced the cell viability of non-cancer HEK 293 cell lines in a concentration-dependent manner (see Figures 5A and B). At 10, 5, and 2.5 µM, there was a decline in

cell viability which may show the toxicity of IMA on non-cancer cells. At lower concentrations, IMA did not eradicate or affect the viability of non-cancer cells, but this shows that IMA may be toxic at higher concentrations to both cancer and non-cancer cells. Therefore, optimization of the exact activity of IMA on cancer and non-cancer is required to be investigated in the future. DMSO (0.1 %) was used as a negative control. The activity of DMSO may depend on the type of cell lines and it may either slow down cell proliferation or promote cell proliferation. Therefore, based on the cell antiproliferative results, the decreasing concentrations of DMSO did not affect the biological activity of IMA on the cells or contributed to IMA activity.

IMA exhibited anti-proliferative effects on RMG-1 cell lines (see Figures 6 A and B). In real-time cell viability analysis, IMA exhibited anticancer activity, as inhibition of cell proliferation was observed over 48-hour treatments (see figure 6B). The same trend from MDA-MB 231 cells results was observed on RMG-1. The results in figures 7i and iii, exhibited that IMA induced cell apoptosis on RMG-1 cell lines at IC_{50} concentration (2.3 µM). It can be supported by the upregulation of the BAX gene and the downregulation of anti-Bcl2. Caspase 3/7 activity (figure 8) after treatment with IMA was highly expressed in comparison with etoposide. This correlates with the apoptosis and cell cycle regulation results. Cell cycle arrest was observed in the S phase with a high number of cells as compared to the other phases (figure 7ii and iv). The cell cycle arrest in the S phase only may reveal that IMA has the properties to inhibit damaged DNA to replicate, hence cells were inhibited from progression within 24 hours of treatment. Therefore, IMA may possess anticancer effects on RMG-1 cancer cell lines, and it may be a promising agent to develop cancer therapies targeting the synthesis phase. P21 was slightly upregulated on RMG-1 cells and highly upregulated on MDA-MB 231 cells (figure 4). P21 is known to enhance apoptosis in the absence of p53 through other complex mechanisms (**24**). The biological activity of IMA may differ based on the type of cell lines and period of exposure.

Conclusion

This study has reported the first findings of the antiproliferative effect of IMA in cancer cell lines. IMA has been shown to inhibit cell proliferation of breast and ovarian cancer cells,

modulate the cell cycle arrest, and induced cell death through the intrinsic apoptotic pathway. With the activation of the apoptotic genes such as BAX, expression of caspase 3/7 pathway, and p21. IMA may be considered a promising candidate for the development of anticancer drugs either for its cytotoxic or cytostatic effect with proper regulation on the non-cancer cells. Furthermore, IMA requires to be further studied more to clearly understand its mechanism of action. It will also serve the purpose to evaluate IMA's optimum cytotoxic effect within various time points. In the future, protein expression will be evaluated including other genes involved in the cell cycle arrest and apoptosis such as pRB, p16.

List of abbreviations

Iso-mukaadial acetate (IMA); Dimethyl sulfoxide (DMSO); Propidium Iodide (PI); Tumour Protein p53 (*TP53*); Cyclin-dependent kinase inhibitor 1A (CDKN1A or p21); Bcl-2associated X (BAX); B-cell lymphoma 2 (Bcl2); Retinoblastoma-binding protein 6 (RBBP6); Cyclin dependent kinase 2 (CDK2); Deoxyribonucleic acid (DNA);
Retinoblastoma protein (pRB); Cyclin-dependent kinase inhibitor 2A (CDKN2A) or p16; Glyceraldehyde 3-phosphate dehydrogenase (GAPDH).

Declaration

Ethics approval and consent to participate: Not applicable.

Author Contributions: Formal analysis, P.P Raphela-Choma and M.S Choene; Funding acquisition, M.S Choene; Investigation, Portia Raphela-Choma; Methodology, P.P Raphela-Choma; Resources, M.S Choene; Supervision, M.B.C Simelane and M.S Choene; Writing – original draft, P.P Raphela-Choma; Writing – review & editing, M.B.C Simelane and M.S Choene.

Funding: Authors would like to acknowledge the South African National Research Foundation.

Consent for publication: Not applicable.

Competing interests: Authors declare that they have no competing interests.

Availability of data and material: The data produced are already at the University of Johannesburg, South Africa, in the form of a dissertation.

Acknowledgements: Not applicable.

References

1. Luo, J., Hu, Y., and Wang, H. Ursolic acid inhibits breast cancer growth by inhibiting proliferation, inducing autophagy and apoptosis, and suppressing inflammatory responses via the PI3K/AKT and NF-κB signaling pathways. Experimental and Therapeutic Medicine. 2017 14(4), 3623-3631.
2. Iqbal, J., Abbasi, B.A., Ahmad, R., Mahmood, T., Kanwal, S., Ali, B., Khalil, A.T., Shah, S.A., Alam, M.M., and Badshah, H. Ursolic acid a promising candidate in the therapeutics of breast cancer: Current status and future implications. Biomedicine and Pharmacotherapy. 2018, 108, 752-756.
3. Sak, K. In vitro cytotoxic activity of flavonoids on human ovarian cancer cell lines. Cancer Science and Research. Open access. 2015, 2(1), 1-13.
4. Pistritto, G., Trisciuoglio, D., Ceci, C., Garufi, A., and D'Orazi2, G. Apoptosis as anticancer mechanism: Function and dysfunction of its modulators and targeted therapeutic strategies. Aging Albany. 2016, 8(4), 603-619.
5. Benarba, B. and Pandiella, A. Colorectal cancer and medicinal plants: Principle findings from recent studies. Biomedicine & Pharmacotherapy, 2018,107, 408423.
6. Majolo, F., Delwing, L.K.D.O.B., Marmitt, D.J., Bustamante-Filho, I.C. and Goettert, M.I. Medicinal plants and bioactive natural compounds for cancer treatment: Important advances for drug discovery. Phytochemistry Letters, 2019, 31,196-207.
7. Barata, A.M., Rocha, F., Lopes, V. and Carvalho, A.M. Conservation, and sustainable uses of medicinal and aromatic plants genetic resources on the worldwide for human welfare. Industrial Crops and Products,2016, 88, 8-11.
8. Liao, L., Liu, C., Xie, X., Zhou, J. Betulinic acid induces apoptosis and impairs migration and invasion in a mouse model of ovarian cancer. Journal of Food Biochemistry, 2020, 1-4.

9. Mitra, S., and Dash, R. Natural Products for the Management and Prevention of Breast Cancer. Review Article. Evidence-Based Complementary and Alternative Medicine. 2018, 23.
10. Msomi, N.Z., Shode, F.O., Pooe, O.J., Mazibuko-Mbeje, S., and Simelane, M.B.C. Iso-mukaadial acetate from Warburgia salutaris enhances glucose uptake in the L6 rat myoblast cell line. Biomolecules. 2019, 9(10), 520.
11. Nyaba, Z.N., Murambiwa, P., Opoku, A.R., Mukaratirwa, S., Shode, F.O., and Simelane, M.B.C. Isolation, characterization and biological evaluation of a potent anti-malarial drimane sesquiterpene from Warburgia salutaris stem bark. Malaria Journal. 2018, 17(1), 296.
12. Opoku, F., Govender, P.P., Pooe, O.J., 2 and Simelane, M.B.C. Evaluating isomukaadial acetate and ursolic acid acetate as Plasmodium falciparum. Hypoxanthine-Guanine-Xanthine Phosphoribosyl-transferase Inhibitors. Biomolecules. 2019, 9(12), 861.
13. Maroyi, A. The genus warburgia: A review of its traditional uses and pharmacology. Pharmaceutical Biology. 2014, 52(3), 378-391.
14. Kotina, E.L., Van Wyk, B.E., Tilney, P.M. Anatomy of the leaf and bark of Warburgia salutaris (Canellaceae), an important medicinal plant from South Africa. South African Journal of Botany. 2014, 94, 177-181.
15. Soyingbe, O.S., Mongalo, N.I., and Makhafola, T.J. In vitro antibacterial and cytotoxic activity of leaf extracts of Centella asiatica (L.) Urb, Warburgia salutaris (Bertol. F.) Chiov and Curtisia dentata (Burm. F.) C.A.Sm -medicinal plants used in South Africa. BMC Complementary and Alternative Medicine. 2018, 18,315.
16. Choudhari, A.S., Mandave, P.C., Deshpande3, M., Ranjekar, P., and Prakash, O. Phytochemicals in Cancer Treatment: From Preclinical Studies to Clinical Practice. Review Article. Frontiers in Pharmacology. 2020, 10,1-17.
17. Moodley, R., Koorbanally, N.E., and Jonnalagadda, S.B. Structure and antioxidant activity of phenolic compounds isolated from the edible fruits and stem bark of Harpephyllum caffrum. Part B, pesticides, food contaminants and agricultural wastes. Journal of Environmental Science and Health. 2014, 49(12), 938.

18. Peña-Morán, O.A., Villarreal, M.L., Álvarez-Berber, L., Meneses-Acosta, A. and Rodríguez-López, V., 2016. Cytotoxicity, post-treatment recovery, and selectivity analysis of naturally occurring podophyllotoxins from Bursera fagaroides var. fagaroides on breast cancer cell lines. Molecules,2016, 21(8),1013.
19. Li, Y., Yu, H., Han, F., Wang, M., Luo, Y., and Guo, X., 2018. Biochanin A induces S phase arrest and apoptosis in lung cancer cells. BioMed research international, 2018.
20. Shankar, E., Zhang, A., Franco, D., and Gupta, S. Betulinic Acid-Mediated Apoptosis in HumanProstate Cancer Cells Involves p53 and Nuclear Factor-Kappa B (NF-_B) Pathways. Molecules. 2017, 22, 264.
21. Tiwari, R., Puthli, A., Balakrishnan, S., Sapra, B.K., and Mishra, K.P. Betulinic Acid-Induced Cytotoxicity in Human Breast Tumor Cell Lines MCF-7 and T47D and its Modification by Tocopherol. Cancer Investigation, 2014, 32(8), 402-408.
22. Bačević, K., Lossaint, G., Achour, T.N., Georget, V., Fisher, D. and Dulić, V., 2017. Cdk2 strengthens the intra-S checkpoint and counteracts cell cycle exit induced by DNA damage. Scientific reports, *7*(1),1-14. DOI:10.1038/s41598-017-12868-5.
23. Badmus, J.A., Ekpo, O.E., Hussein, A.A., Meyer, M. and Hiss, D.C., 2019. Cytotoxic and cell cycle arrest properties of two steroidal alkaloids isolated from Holarrhena floribunda (G. Don) T. Durand & Schinz leaves. BMC complementary and alternative medicine, 2019, 19(1),1-9. https://doi.org/10.1186/s12906-0192521-9.
24. Manu, K., Cao, P., Chai, T., Casey, P. and Wang, M. P21cip1/waf1 coordinates autophagy, proliferation and apoptosis in response to metabolic stress. Cancers, 2019, 11(8):1-15.